Direct Measurement of Ion Mobility in a Conducting Polymer

*Eleni Stavrinidou, Pierre Leleux, Harizo Rajaona, Dion Khodagholy, Jonathan Rivnay, Manfred Lindau, Sébastien Sanaur, and George G. Malliaras**

A key difference between organic electronic materials and inorganic ones such as silicon lies in the ability of the former to transport ions with significant mobilities at room temperature. This important property, which arises from the "soft" nature of van der Waals-bonded organics, is leveraged in a variety of devices that utilize mixed electronic/ionic conduction.[1] In electrochromic displays,[2] for example, ions injected from an electrolyte change the color of a polymer film. The dimensional changes that arise from ion injection are used to build mechanical actuators (artificial muscles).[3] Ion redistribution within a film facilitates electronic charge injection from metal electrodes, an effect utilized to achieve efficient electroluminescence in light emitting electrochemical cells.[4,5] Finally, ion diffusion across an interface is used to control the energetics of the heterojunction, thus forming diodes.[6,7] Mixed electronic/ionic conductivity is of particular importance for devices that interface electronics with biology, a subject that is currently attracting a great deal of attention.[8,9] One example is the organic electrochemical transistor (OECT), in which ions from an electrolyte enter a polymer film and change its electronic conductivity.[10] This results in ionic-to-electronic signal transduction, and has found several applications in biosensors.[11] A second example is the organic electronic ion pump (OEIP), in which an electronic current in a conducting polymer film controls the delivery of ions into an aqueous solution.[12] These devices have been used in vivo for drug delivery with unparalleled spatiotemporal resolution.[13]

Despite the emerging importance of ionic transport in organic electronics, very little is known about the fundamentals of ion transport in these materials, and there has not been a concerted effort towards the rational design of materials which simultaneously optimize electronic and ionic transport. Ion transport has been studied in polymer electrolytes such as Nafion using conductivity or diffusion measurements.[14] The simultaneous presence of electronic carriers in mixed conductors, however, greatly complicates the analysis of data and renders these techniques unusable. As a result, even for common materials used in mixed conductor devices, such as poly(3,4-ethylenedioxythiophene) poly(styrenesulfonate) (PEDOT:PSS), ion mobility values are largely unknown. This is in sharp contrast with electronic transport in organics, which has been under intense scrutiny since the 1970s, motivated largely by the application of organics in electrophotography.[15] The time-of-flight technique, which measures the transit of photo-injected carriers through a thick film, played a key role in enabling a better fundamental understanding of electronic transport in organics.[16] This in turn led to the development of state-of-the-art materials, which helped advance the emergence of organic electronics.[17] An equivalent technique for measuring ionic transport would constitute a major step towards the development of mixed conductor materials and devices.

Organic electronic materials are inherently electrochromic, meaning that the presence of free electronic carriers creates states in the optical gap and changes the color of the film.[18] This phenomenon has been used to monitor doping/dedoping effects in conducting polymer films.[19–21] A variety of experimental configurations including injection of ions from an electrolyte and injection or extraction of holes from a metal electrode, have been employed. Depending on the exact geometry, ion or hole transport was the rate-limiting step in the doping/dedoping process. In all of these experiments, however, ions and holes were transported in directions that were perpendicular to each other. This 2D geometry made it difficult to calculate the field inside the polymer film and to determine the ion mobility.

In this communication, we report measurements on planar electrolyte/PEDOT:PSS junctions, in which the 1D geometry of the experiment allows a straightforward estimation of the ion drift mobility. The geometry of the experiment is shown in **Figure 1**a. A PEDOT:PSS film, deposited on a parylene-coated glass substrate, was coated with a layer of SU-8. The latter served as an insulating ion barrier, and prohibited ion injection into the PEDOT:PSS film from the top. Using photolithography, a well was created in the SU8/PEDOT:PSS stack and filled with an electrolyte, forming a planar electrolyte/PEDOT:PSS junction with an area A of 16 mm × 400 nm (width × thickness of the PEDOT:PSS film). A Ag/AgCl counter electrode was immersed into the electrolyte, and a Au pad provided contact with the PEDOT:PSS film, positioned at a distance L = 32 mm from the electrolyte interface. Ag/AgCl was chosen as the counter electrode to ensure a negligible potential drop at its interface with the electrolyte. The experiment was carried out by applying a positive bias at the Ag/AgCl electrode (which drove cations from the electrolyte into the PEDOT:PSS film leading to its gradual

E. Stavrinidou, P. Leleux, H. Rajaona, Dr. D. Khodagholy, Dr. J. Rivnay, Dr. S. Sanaur, Prof. G. G. Malliaras
Department of Bioelectronics
Ecole Nationale Supérieure des Mines
CMP-EMSE, MOC, 13541 Gardanne, France
E-mail: malliaras@emse.fr
Prof. M. Lindau
Department of Applied and Engineering Physics
Cornell University
Ithaca, NY 14853, USA

DOI: 10.1002/adma.201301240

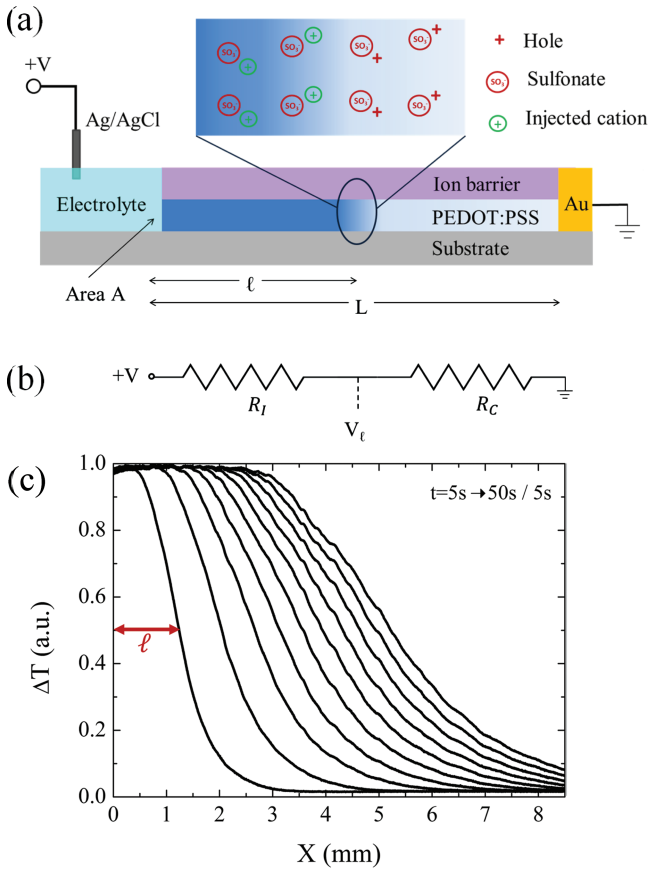

Figure 1. a) Schematic of the device indicating the charge distribution around the dedoping front according to the model (not to scale), the drift length, ℓ, of injected ions, the total length, L, of the PEDOT:PSS film, and the area, A, of the electrolyte/conducting polymer junction. b) The equivalent circuit diagram, where R_I and R_C are the equivalent resistors corresponding to the dedoped and the still-doped parts of the PEDOT:PSS film, respectively, and V_ℓ is the voltage at ℓ. c) The evolution of the dedoping front in PEDOT:PSS during the injection of potassium cations, where ΔT is the change of transmitted light intensity with respect to the zero bias state. Time $t = 0$ corresponds to the application of a bias voltage, and $x = 0$ mm corresponds to the interface with the electrolyte. The applied bias was 2 V. The red arrow indicates the drift length of ions at $t = 5$ s.

dedoping) while simultaneously measuring the current flow in the device and the electrochromic changes associated with the propagation of the dedoping front. The dedoping was found to be reversible and the film returned to its doped state upon removal of the applied bias. We found a few dedope/re-dope cycles were required in order to reach a reproducible temporal dependence of the current during a dedoping cycle. This is consistent with previous measurements in conducting polymer films and has been attributed to hydration of the polymer film during the first cycles.[22] All the data discussed from this point on were obtained on films that were appropriately cycled to reach this reproducible behavior. It should be noted that the well was made large enough to ensure that ion depletion of the electrolyte was negligible during the experiment.

The propagation of the dedoping front was quantified by measuring the optical transmission of the PEDOT:PSS film. Typical data for potassium cations are shown in Figure 1c. The data correspond to the change of transmitted light intensity (ΔT) with respect to the zero bias state. Time $t = 0$ s corresponds to the application of a bias, and $x = 0$ mm corresponds to the electrolyte/conducting polymer interface. The dedoping profiles exhibit a clear saturation, indicating that a maximum level of dedoping was reached. The leading front exhibits the typical shape associated with diffusive spread of the carriers. The drift length, ℓ, of ions was obtained from the position of half-maximum change in ΔT, as indicated in Figure 1c.

The data obtained from these experiments were further analyzed using a simple analytical model (see Supporting Information), based on the following physical mechanism: PEDOT:PSS is a degenerately doped organic semiconductor, in which the semiconductor chain (PEDOT) is *p*-type doped due to the presence of uncompensated sulfonate anions on the PSS chain (PSS is added in excess, and only a fraction of its sulfonate anions is compensated by holes and hence contributes to doping. These are the sulfonate anions we consider here). When a positive bias is applied to the Ag/AgCl electrode, cations are injected into the PEDOT:PSS film and drift towards the Au electrode, while holes drift towards the Au electrode. Charge neutrality implies that cation injection is balanced by hole extraction, meaning that as the sulfonate anions are compensated by the injected cations, the excess holes are swept away by the hole drift current. The 1D geometry of the experiment permits the direct observation of the front between the dedoped part of the film, where the current is dominated by cation drift, and the still-doped part of the film, where the current is dominated by hole drift. The dedoped part extends a distance ℓ from the interface with the electrolyte, where ℓ is the drift length of the injected cations. Accordingly, we model the partially dedoped PEDOT:PSS film as two resistors in series (Figure 1b) where R_I corresponds to the dedoped part and R_C corresponds to the still doped part. We assume that the cation mobility in the film is lower than that of holes, hence the conductivity of the dedoped part of the film is lower than that of the doped part of the film. Based on these assumptions one can show that $V(\ell) \approx V$, meaning that the applied potential drops exclusively on the dedoped part (an assumption validated by numerical simulations, see Supporting Information). Accordingly, we find that the drift length increases with time as:

$$\ell^2 = 2\mu V t \tag{1}$$

where V is the applied bias and t is time, and μ is the mobility of the injected cations. The current density, j, decreases with time as:

$$j = \frac{e P \sqrt{2\mu V}}{2\sqrt{t}} \tag{2}$$

where e is the elementary charge and P is the injected cation density in the dedoped part of the film. The latter is assumed to be equal to the density of the sulfonate ions, as indicated in the schematic of Figure 1a.

Equation 1 allows a straightforward determination of the cation drift mobility from the dedoping fronts. The solid circles in **Figure 2**a show the temporal evolution of the drift length of potassium cations in a PEDOT:PSS film. The line is a fit of the model, yielding a potassium mobility of 1.4×10^{-3} cm^2 V^{-1} s^{-1}. This value is higher than the electrophoretic mobility of

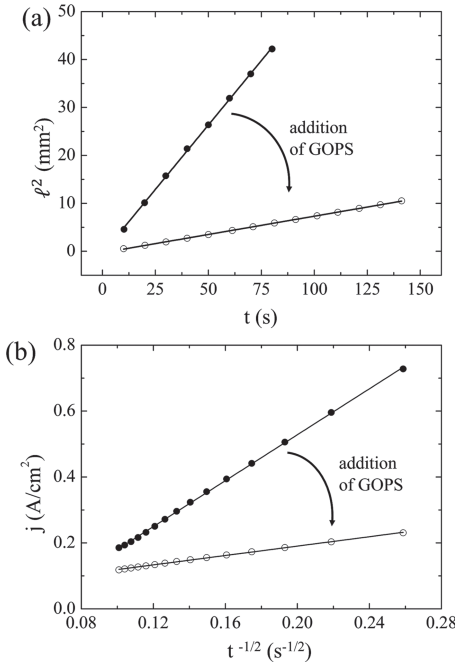

Figure 2. Temporal evolution of the drift length, ℓ, of potassium cations (a) and of the corresponding current density, ℓ, (b) in PEDOT:PSS and in crosslinked PEDOT:PSS films.

potassium cations in bulk water at the limit of infinite dilution (7.6×10^{-4} cm^2 V^{-1} s^{-1}),[23] implying first and foremost that the film is highly hydrated. Mobilities close to water are known in gels as well as in polymers such as Nafion[24] and PSS[25] and are associated with extensive hydration which leads to the formation of channels of water that occupy most of the film volume. Indeed, the volume increase during swelling of a PEDOT:PSS film that was appropriately cycled was measured using optical profilometry to be 155% (see Supporting Information).

Exactly how water is distributed within (and how it alters) the physical microstructure of PEDOT:PSS films is not fully understood. In PEDOT:PSS dispersions, PEDOT and PSS form a poly-ion complex. The polyanion (PSS) is in excess and forms a PSS-rich shell around a poly-ion rich core, yielding colloidal gel particles in suspension.[26] After proper shearing and sonication, such colloidal particles are known to be in the range of 5–30 nm.[27] A commonly agreed model of the film microstructure is the physical interconnection and flattening of these colloidal gel particles upon film casting, whereby the channels for ion/electron motion are predetermined by the colloids that were in suspension.[27,28] Addition of a co-solvent, such as the ethylene glycol in this work, is thought to invert or homogenize the content of the colloidal particles, bringing more PEDOT to the surface, and enhancing the molecular scale ordering of the poly-ion complex.[26,27] Thus, in both dry and hydrated films cast from these suspensions, PEDOT-rich regions form a more continuous interconnected network, allowing for efficient electronic transport.[26,29] It has been shown that the PSS-rich regions in colloidal particles are in the range of 5–15 nm.[27,30] According to this picture, and given that hydration is expected to progresses largely in the PSS phase, we suggest that the ion-transport pathways in PEDOT:PSS films are comprised of larger (tens of nanometers) water channels in the PSS-rich phase, feeding into smaller pathways through complexed PEDOT:PSS. The experimental geometry used here, therefore, resembles capillary electrophoresis, in which, in addition to electrophoretic ion migration, an electroosmotic flow can be established.[31] Indeed, PSS-lined microfluidic channels have shown to support electroosmotic flow[32] with a mobility of 4×10^{-4} cm^2 V^{-1} s^{-1}. Hence, the measured ionic mobility should be interpreted as the sum of the electrophoretic and electroosmotic mobilities in the transport pathways.

One way to modify the transport pathways is to crosslink the film and therefore decrease its ability to uptake water. This was achieved through the addition of the crosslinker 3-glycidoxypropyltrimethoxysilane (GOPS), which reduced the swelling of the PEDOT:PSS film to only 35% and accordingly reduced the ion mobility (Figure 2a, open circles). The fit of the model (Figure 2a, line through open circles) reveals that the crosslinker decreased potassium mobility by an order of magnitude, to 1.9×10^{-4} cm^2 V^{-1} s^{-1}. It should be noted that the electrical conductivity of the dry films decreased only by 45% with the addition of the crosslinker.

The model can be further validated by analyzing the time dependence of current density, j, which provides an estimate of the injected ion density, P, in the film (Figure 2b). The data for PEDOT:PSS films with and without crosslinker are well fitted by Equation 2. As for the drift length, the model predicts the correct time dependence of current density, indicating that it captures the essential physics of ion injection in conducting polymers. For films with and without crosslinker the fits yielded ion densities of 5.9×10^{20} cm^{-3} and 3.2×10^{20} cm^{-3}, respectively. A key assumption of the model is that the injected cations compensate the sulfonate anions, hence P is equal to the sulfonate anion density. The latter is estimated to be of the order of $3–4 \times 10^{20}$ cm^{-3}, assuming a sulfonate group for every 3–4 PEDOT monomer units,[27] a 1:2.5 w/w ratio of PEDOT to PSS (for Clevios PH500), and a density of 1 g/cm^3 for the film. The good agreement between the obtained values of P and sulfonate anion density lends additional support to the model.

Furthermore, we can estimate the hole mobility in PEDOT:PSS. According to the model, the extrapolated current at $t = 0$ s is dominated by hole transport (resistor R_C is dominant in the equivalent circuit diagram of Figure 1b), and hence reflects the hole conductivity in the film. Assuming that the hole density (which is equal to the sulfonate density) is equal to the injected ion density, we obtain a hole mobility of approximately 0.06 cm^2 V^{-1} s^{-1} for both the pristine and the crosslinked films. These values are considerably higher than the values determined for the potassium mobility, which is consistent with the key assumption of the model, namely that the conductivity of the dedoped part of the film is lower than that of the doped part of the film. It should be noted that the hole mobility can be independently determined by analyzing the response of OECTs to constant gate current.[10] We fabricated devices made from the same PEDOT:PSS film and obtained a hole mobility of 0.01 cm^2 V^{-1} s^{-1} (see Supporting Information). This value is in good agreement with the one estimated by ion injection, which further supports for the validity of the model.

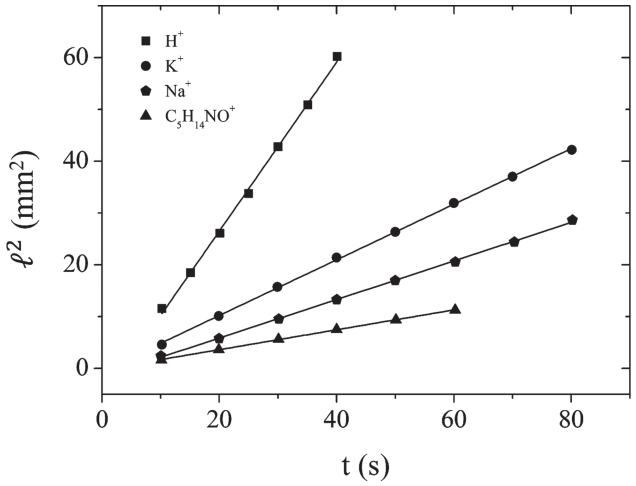

Figure 3. Temporal evolution of the drift length, ℓ, of various cations in PEDOT:PSS during a dedoping cycle.

The measurements above were carried out in electrolytes with a concentration of 10 mM. Measurements were also conducted with electrolyte concentrations spanning two orders of magnitude from 1 mM to 100 mM. Saturated optical transmission profiles were observed and Equation 1 was found to hold in this concentration range (see Supporting Information), allowing the mobility to be determined. A slight increase of the mobility with concentration was observed, indicating that mild heating of the film might be taking place.[33] In electrolytes with concentrations of 1 M and higher, ℓ^2 exhibited a sub-linear time dependence, which is not captured by our model. Such a deviation can be described by strong ion-ion interactions, which render ion transport more dependent on the coupling to the counter ions and invalidate the assumption that the ions are fully dissociated. Ion concentrations lower than 1 mM were not investigated, as the potential drop at the electrolyte becomes non-negligible.

We subsequently evaluated the transport of different cations in PEDOT:PSS films. **Figure 3** shows the drift length of protons, potassium, sodium and choline ($C_5H_{14}NO^+$, molar mass of 104.62 g/mol) cations, at a concentration of 10 mM. The data for all ions follow the ℓ^2 vs. t dependence, allowing the determination of mobilities, shown in **Table 1**. As with potassium, the mobilities of these ions in PEDOT:PSS were found to be a bit higher than the electrophoretic mobilities measured in bulk water, indicating that electroosmosis plays a role in ion transport in PEDOT:PSS. It should be noted that Na^+ shows a lower mobility than K^+, consistent with a larger hydration sphere.[23] These results emphasize that PEDOT:PSS is an efficient ion transporter for applications in bio-interfacing, where the film is in direct contact with and hence takes up water. However, PEDOT:PSS is not stable over long times to immersion in water and dissolves or delaminates upon agitation. Addition of a crosslinker such as GOPS[34] or the use of a vapor-phase deposited PEDOT[35] have been used as alternatives that enable long-term operation of devices. Our work implies that such approaches trade, to a certain extent, ion mobility for stability, and that further understanding and engineering of the polymer microstructure is needed to allow co-optimization of stability, electronic transport and ion transport.

Table 1. Mobility of various cations in PEDOT:PSS (measured with 10 mM solutions), in water, at the limit of infinite dilution.

Ion	Mobility in PEDOT:PSS [$cm^2 V^{-1} s^{-1}$]	Electrophoretic mobility in bulk water [$cm^2 V^{-1} s^{-1}$]
H^+	$3.9 \pm 0.2 \times 10^{-3}$ ($N = 3$)	3.6×10^{-3} (from ref.[23])
K^+	$1.4 \pm 0.2 \times 10^{-3}$ ($N = 8$)	7.6×10^{-4} (from ref.[23])
Na^+	$9.3 \pm 0.4 \times 10^{-4}$ ($N = 3$)	5.2×10^{-4} (from ref.[23])
$C_5H_{14}NO^+$	$4.5 \pm 0.4 \times 10^{-4}$ ($N = 3$)	3.9×10^{-4} (calculated from ref.[36])

Of particular interest is the fact that choline, an organic cation that is an essential nutrient, is transported efficiently in PEDOT:PSS. This implies that the size of water channels in PEDOT:PSS is larger than the size of the choline ion, and prompts the question of what the maximum ion size is for efficient transport through this material. This question has important technological ramifications for the design of OEIPs, which employ electrophoretic transport of ions in a conducting polymer film. It has been shown that these devices can deliver a variety of neurotransmitters,[13] including acetylcholine.[37] The method described here can help answer this question by quantifying the mobility of biologically-relevant ions.

In this Communication we focused on ions that are injected in the film from aqueous solutions, which is of particular interest to bio-interfacing. In other applications of mixed ionic/electronic transporters, such as in light-emitting electrochemical cells, the organic layer is not in contact with an electrolyte and hence ion transport occurs in a dry film. This limit can also be approached with the method described here, if an ionic liquid is used to supply the ions instead of an electrolyte solution. As solvent-free ion solutions, ionic liquids can inject non-solvated ions into a conducting polymer, which creates an opportunity to study ion transport in a different regime. Ionic liquids have already been used as a source of mobile ions in ionic polymer transducers.[38] Alternatively, a solid electrolyte can be used as a source of ions in order to avoid hydration and allow a measurement of ion transport in a dry film. The results presented above show that mobility decreases when hydration is decreased, which brings up the question of what is the "sensitivity" of this method. Equation 1 shows that for a mobility of 10^{-8} $cm^2 V^{-1} s^{-1}$ and an applied bias of 2 V, the front moves 2 µm in the first 1 s of the measurement. Given that PEDOT:PSS can be patterned with <<1 µm line edge roughness using photolithography,[39] the method described here appears to be suitable for such measurements. Finally, the model can be easily adapted to other configurations such as the doping of intrinsic organic semiconductors, or the dedoping of *n*-type organic semiconductors, broadening the matrix of materials in which ion transport can be measured. As interest in organic electronic materials that support both electronic and ionic transport increases, the method developed here will play an important role in establishing structure vs. ion transport properties relationships.

Experimental Section

Planar junctions were fabricated using standard microfabrication techniques. The fabrication started with the deposition of a 2 µm-thick parylene-C film (Specialty Coating Systems) on a glass substrate (26 mm × 76 mm), and the subsequent spin-coating of a commercial solution of PEDOT:PSS (Clevios - PH500), with the addition of 20% anhydrous ethylene glycol and DBSA (50 µm in 25 mL of solution). The parylene film, which was mildly etched with oxygen plasma (100 W for 2 min in a Reactive Ion Etcher, Oxford) just before the deposition of PEDOT:PSS, was used to prevent delamination of the PEDOT:PSS film from the substrate. The thickness of the PEDOT:PSS films used in this study was 400 nm, achieved with multiple depositions followed by a soft bake at 90 C for 1 min between each deposition. The films were then baked at 90 °C for 20 min and finally at 140 °C for 40 min and then rinsed in deionized water for 30 min to remove low molecular weight additives. A 100 nm gold electrode was deposited on one side of the film using a shadow mask. A 40 µm-thick SU-8 film was spin-coated on top of the PEDOT:PSS film to serve as an ion barrier. After a post-exposure bake, it was developed according to the manufacturer's specifications to open a well of 16 mm × 5 mm. PEDOT was removed mechanically, using a swab dipped in acetone, and a polydimethylsiloxane rim was placed on top of the SU-8 well to confine 1.5–2 mL of electrolyte. The area of the junction was equal to 400 nm × 16 mm, and the length of the PEDOT:PSS film between the electrolyte and the Au contact was 32 cm. It should be noted that conductivity measurements on test samples showed that the processing of the SU-8 film did not affect the electrical properties of the PEDOT:PSS. Finally, a Ag/AgCl electrode was immersed in the electrolyte. Experiments were also performed on films that were crosslinked with the addition of 1 wt% of GOPS in the PEDOT:PSS solution just before spin coating.

The device-to-device reproducibility was found to be better than 15%, which permitted a pristine device to be used for each type of electrolyte. The latter were freshly made before each measurement by adding the appropriate amounts of HCl, KCl, NaCl, and choline chloride (Sigma–Aldrich) in deionized water. Dedoping was achieved by applying a positive bias to the Ag/AgCl electrode. The dedoping front was not allowed to reach the Au electrode. The device was then short-circuited to return to its doped state. This defined one cycle. The current vs. time curves were found to reach a reproducible behavior after the first 2–3 cycles. The mobility values were found to be independent of applied bias (within the device-to-device reproducibility error) in the range of 2–4 V. The measurements were conducted on an inverted Carl Zeiss Axio Observer Z1, and time lapse images were recorded in the bright-field mode with a 1× objective. The images were corrected to assure uniform light intensity throughout the field of view. Grey level profiles along the *x* direction (from the electrolyte to the Au electrode) were calculated using a custom MatLab program. The drift length of the cations was calculated from the position of half-maximum intensity change (ΔT). The current flowing through the device was recorded with a Keithley 2612A source-measure unit connected to a computer running custom LabView software.

Supporting Information

Supporting Information is available from the Wiley Online Library or from the author.

Acknowledgements

This work was supported by grants from ANR, CG-13, région PACA, Microvitae Technologies, and Marie CURIE. The authors acknowledge funding from the Partner University Fund (a program of French American Cultural Exchange). We would like to thank Bjorn Winther-Jensen (Monash University) and Olle Inganäs (Linköping University) for fruitful discussions.

Received: March 18, 2013
Revised: April 24, 2013
Published online: June 20, 2013

[1] J. M. Leger, *Adv. Mater.* **2008**, *20*, 837.
[2] R. J. Mortimer, A. L. Dyer, J. R. Reynolds, *Displays* **2006**, *27*, 2.
[3] E. Smela, *MRS Bull.* **2008**, *33*, 197.
[4] Q. Pei, G. Yu, C. Zhang, Y. Yang, A. J. Heeger, *Science* **1995**, *269*, 1086.
[5] J. C. deMello, N. Tessler, S. C. Graham, R. H. Friend, *Phys. Rev. B* **1998**, *57*, 12951.
[6] C. H. W. Cheng, M. C. Lonergan, *J. Am. Chem. Soc.* **2004**, *126*, 10536.
[7] D. A. Bernards, S. Flores-Torres, H. D. Abruna, G. G. Malliaras, *Science* **2006**, *313*, 1416.
[8] M. Berggren, A. Richter-Dahlfors, *Adv. Mater.* **2007**, *19*, 3201.
[9] R. M. Owens, G. G. Malliaras, *MRS Bull.* **2010**, *35*, 449.
[10] D. A. Bernards, G. G. Malliaras, *Adv. Funct. Mater.* **2007**, *17*, 3538.
[11] P. Lin, F. Yan, *Adv. Mater.* **2012**, *24*, 34.
[12] J. Isaksson, P. Kjall, D. Nilsson, N. D. Robinson, M. Berggren, A. Richter-Dahlfors, *Nat. Mater.* **2007**, *6*, 673.
[13] D. T. Simon, S. Kurup, K. C. Larsson, R. Hori, K. Tybrandt, M. Goiny, E. W. H. Jager, M. Berggren, B. Canlon, A. Richter-Dahlfors, *Nat. Mater.* **2009**, *8*, 742.
[14] B. Smitha, S. Sridhar, A. A. Khan, *J. Membr. Sci.* **2005**, 259, *10*.
[15] P. M. Borsenberger, D. S. Weiss, *Organic Photoreceptors for Xerography*, Marcel Dekker, Inc., New York **1998**.
[16] H. Bässler, *Phys. Status Solidi B* **1993**, *175*, 15.
[17] G. Malliaras, R. Friend, *Phys. Today* **2005**, *58*, 53.
[18] R. H. Friend, *Synth. Met.* **1992**, *51*, 357.
[19] K. Aoki, T. Aramoto, Y. Hoshino, *J. Electroanal. Chem.* **1992**, *340*, 127.
[20] T. Johansson, N.-K. Persson, O. Inganäs, *J. Electrochem. Soc.* **2004**, *151*, E119.
[21] X. Wang, E. Smela, *J. Phys. Chem. C* **2009**, *113*, 369.
[22] X. Wang, E. Smela, *J. Phys. Chem. C* **2009**, *113*, 359.
[23] P. Atkins, J. de Paula, *Physical Chemistry*, Oxford University Press, Oxford, UK **2006**.
[24] P. Knauth, E. Sgreccia, A. Donnadio, M. Casciola, M. L. Di Vona, *J. Electrochem. Soc.* **2011**, *158*, B159.
[25] K. Tybrandt, R. Forchheimer, M. Berggren, *Nat. Commun.* **2012**, *3*, 871.
[26] H. Okuzaki, presented at 2012 19th International Workshop on Active-Matrix Flatpanel Displays and Devices (AM-FPD), Kyoto, Japan, July 2012.
[27] A. Elschner, S. Kirchmeyer, W. Lövenich, U. Merker, K. Reuter, in *PEDOT, Principles and Applications of an Intrinsically Conductive Polymer*, CRC Press, Boca Raton, FL, USA **2010**, 113.
[28] A. M. Nardes, M. Kemerink, R. A. J. Janssen, J. A. M. Bastiaansen, N. M. M. Kiggen, B. M. W. Langeveld, A. J. J. M. van Breemen, M. M. de Kok, *Adv. Mater.* **2007**, *19*, 1196.
[29] S. Ashizawa, R. Horikawa, H. Okuzaki, *Synth. Met.* **2005**, *153*, 5.
[30] P. C. Jukes, S. J. Martin, A. M. Higgins, M. Geoghegan, R. A. L. Jones, S. Langridge, A. Wehrum, S. Kirchmeyer, *Adv. Mater.* **2004**, *16*, 807.
[31] R. Weinberger, *Practical Capillary Electrophoresis, 2nd Ed.*, Academic Press, San Diego, CA, USA **2002**.
[32] S. L. R. Barker, M. J. Tarlov, H. Canavan, J. J. Hickman, L. E. Locascio, *Anal. Chem.* **2000**, *72*, 4899.
[33] W. Ding, M. J. Thornton, J. S. Fritz, *Electrophoresis* **1998**, *19*, 2133.

[34] D. Khodagholy, T. Doublet, M. Gurfinkel, P. Quilichini, E. Ismailova, P. Leleux, T. Herve, S. Sanaur, C. Bernard, G. G. Malliaras, *Adv. Mater.* **2011**, *23*, H268.
[35] B. Winther-Jensen, K. West, *React. Funct. Polym.* **2006**, *66*, 479.
[36] B. Ng, P. H. Barry, *J. Neurosci. Methods* **1995**, *56*, 37.
[37] K. Tybrandt, K. C. Larsson, S. Kurup, D. T. Simon, P. Kjall, J. Isaksson, M. Sandberg, E. W. H. Jager, A. Richter-Dahlfors, M. Berggren, *Adv. Mater.* **2009**, *21*, 4442.
[38] M. D. Bennett, D. J. Leo, *Sens. Actuators A* **2004**, *115*, 79.
[39] J. A. DeFranco, B. S. Schmidt, M. Lipson, G. G. Malliaras, *Org. Electron.* **2006**, *7*, 22.